



OPEN

Three-dimensional printing model-assisted single-port laparoscopic multiple myomectomy: a randomized controlled trial

Yuan-Hong Li, Ning Xu✉, Yuan-Qin Gou, Meng-Xi Li & Min Li

Multiple uterine fibroids present significant surgical challenges in single-port laparoscopic myomectomy, particularly regarding optimal removal sequence and surgical planning. Three-dimensional (3D) printing technology offers potential advantages for preoperative planning and intraoperative guidance. We conducted a single-center, randomized controlled trial comparing 3D printing model-assisted single-port laparoscopic myomectomy with conventional surgery in women with multiple uterine fibroids. The primary endpoints were total operative time and estimated blood loss. Secondary endpoints included surgeon workload assessment using the NASA Task Load Index (NASA-TLX), patient satisfaction, surgical complications, and long-term follow-up outcomes including fibroid residual and recurrence rates. Patients were randomly assigned 1:1 to receive either 3D model-assisted surgery or conventional surgery using computer-generated randomization with concealed allocation. Sample size was calculated based on an expected 20-minute reduction in operative time with 80% power and $\alpha = 0.05$. Of 140 patients assessed for eligibility, 133 were randomized and 110 completed the per-protocol analysis (55 in each group). In the per-protocol analysis of 110 patients, the 3D model group had significantly shorter total operative time (mean difference, 25.7 min; 95% confidence interval [CI], 17.7 to 33.7; $P = 0.001$) and modestly reduced estimated blood loss (mean difference, 24.4 ml; 95% CI, 5.1 to 43.7; $P = 0.050$). The 3D model group also showed significant improvements in surgeon workload scores (mean difference, 10.1 points; 95% CI, 6.7 to 13.6; $P < 0.001$) and patient satisfaction (mean difference, 1.8 points; 95% CI, 1.5 to 2.1; $P < 0.001$). Hospital stay duration was similar between groups (4.5 ± 0.3 vs. 4.4 ± 0.3 days; $P = 0.100$). At 1-year follow-up, fibroid recurrence rates were lower in the 3D model group (1.8% vs. 12.7%; $P = 0.060$), and immediate postoperative residual fibroid rates were reduced (1.8% vs. 7.3%; $P = 0.363$). No conversions to open surgery occurred in either group, and complication rates were similar (5.5% vs. 14.5%; $P = 0.202$). Surgical plan adherence analysis demonstrated significantly higher protocol adherence in the 3D model group (87.3% vs. 65.5% exact sequence match; $P = 0.002$). In this single-center trial, 3D printing model-assisted single-port laparoscopic myomectomy significantly improved surgical efficiency and reduced surgeon workload while maintaining excellent safety profiles. The 3D model group demonstrated significantly higher surgical plan adherence compared with conventional planning. While favorable trends were observed in fibroid residual and recurrence outcomes, these findings did not achieve statistical significance and should be interpreted as hypothesis-generating. These results require validation in multicenter trials before broader clinical implementation.

Trial registration: This trial was retrospectively registered in the Chinese Clinical Trial Registry (ChiCTR) under the registration number ChiCTR2500112904, with the first registration on November 20, 2025 (<https://www.chictr.org.cn/showproj.html?proj=287706>).

Keywords Three-dimensional (3D) printing, Single-port laparoscopic myomectomy, Multiple myomectomy

Uterine fibroids affect 20–40% of reproductive-age women and represent the most common indication for hysterectomy worldwide¹. For women desiring fertility preservation, myomectomy remains the gold standard

Department of Gynecology, Chengdu Integrated TCM & Western Medicine Hospital, Chengdu 610000, Sichuan, China. ✉email: 609074657@qq.com

treatment, with laparoscopic approaches increasingly preferred over open surgery due to reduced morbidity and faster recovery^{2,3}. However, multiple fibroids present unique surgical challenges, particularly in single-port laparoscopic procedures where instrument maneuverability is limited and optimal fibroid removal sequence becomes critical for surgical success^{4,5}.

The complexity of multiple myomectomy lies not only in the technical aspects of fibroid enucleation but also in strategic surgical planning. The sequence of fibroid removal can significantly impact operative time, blood loss, and the risk of complications⁶. Traditional preoperative imaging, while providing essential anatomical information, offers limited three-dimensional spatial understanding of fibroid relationships and optimal surgical approaches⁷.

Three-dimensional printing technology has emerged as a promising tool for surgical planning across various specialties, offering tangible, patient-specific anatomical models that enhance spatial understanding and facilitate surgical rehearsal^{8,9}. In gynecologic surgery, preliminary reports have suggested potential benefits of 3D printing for complex cases, but randomized controlled evidence remains limited^{10,11}.

The NASA Task Load Index (NASA-TLX) has been validated as an objective measure of surgeon workload, incorporating mental demand, physical demand, temporal demand, performance, effort, and frustration levels¹². This multidimensional assessment provides valuable insights into the cognitive and physical burden associated with different surgical approaches, which may not be captured by traditional outcome measures¹³.

We hypothesized that 3D printing model-assisted surgical planning would improve operative efficiency and reduce surgeon workload in single-port laparoscopic multiple myomectomy. To test this hypothesis, we conducted a randomized controlled trial comparing 3D model-assisted surgery with conventional approaches in women with multiple uterine fibroids.

Methods

Study design and participants

We conducted a single-center, randomized, controlled trial at Chengdu First People's Hospital from March 2024 to November 2024. The study protocol was approved by the institutional review board (IRB approval number: 2024.XJS.003). All participants provided written informed consent before enrollment. This trial was retrospectively registered in the Chinese Clinical Trial Registry (ChiCTR) under the registration number ChiCTR2500112904 and conducted in accordance with the Declaration of Helsinki.

Eligible participants were women aged 18–45 years with multiple uterine fibroids (≥ 2 fibroids) scheduled for laparoscopic myomectomy. Inclusion criteria included: (1) multiple uterine fibroids confirmed by magnetic resonance imaging (MRI), (2) largest fibroid diameter 3–10 cm, (3) desire for fertility preservation, (4) American Society of Anesthesiologists physical status I-II, and (5) ability to provide informed consent. Exclusion criteria included: (1) suspected malignancy, (2) severe adhesions from previous surgery, (3) coagulopathy or bleeding disorders, (4) pregnancy, (5) contraindications to laparoscopic surgery, and (6) inability to complete follow-up assessments.

Sample size calculation

Sample size was calculated based on the primary endpoint of total operative time. Based on pilot data and previous literature¹⁴, we assumed a mean operative time of 100 ± 25 min in the control group and expected a clinically meaningful reduction of 20 min in the 3D model group. With $\alpha=0.05$ (two-sided) and power = 80%, the required sample size was 50 patients per group. Accounting for an estimated 10% dropout rate, we planned to enroll 55 patients per group (total $n=110$).

Randomization and blinding

Patients were randomly assigned 1:1 to either the 3D model group or control group using computer-generated randomization with variable block sizes (4, 6, and 8) stratified by fibroid number (2–3 vs. ≥ 4 fibroids). Allocation concealment was ensured using sequentially numbered, opaque, sealed envelopes prepared by an independent statistician.

Blinding limitations and bias considerations

Due to the nature of the intervention, surgeons and patients could not be blinded to group assignment, representing a significant methodological limitation. This lack of blinding may have introduced performance bias, where surgeons' knowledge of the intervention could influence their surgical technique, decision-making, or effort level. Detection bias may also have occurred, particularly for subjective outcomes such as patient satisfaction and surgeon workload assessment¹⁵. To minimize detection bias, outcome assessors for postoperative complications and data analysts were blinded to group allocation until completion of the statistical analysis. However, the potential impact of unblinded treatment allocation on subjective outcomes should be considered when interpreting results, particularly for patient satisfaction scores and surgeon-reported measures.

Interventions

3D software model-assisted surgical planning

3D model group Patients underwent preoperative 3D software model construction following a standardized 6-step protocol: (1) high-resolution MRI acquisition, (2) medical image segmentation to identify individual fibroids and anatomical structures, (3) 3D software model generation with quality control validation, (4) interactive model review for surgical planning, (5) individualized fibroid removal sequence planning, and (6) preoperative surgical rehearsal and approach documentation¹⁶. The complete process required approximately 15–18 h, with automated processes comprising the majority of time expenditure. Detailed methodology is provided in RESEARCH PROTOCOL S19.

Control group Patients received standard preoperative evaluation using conventional MRI interpretation without 3D model construction. Surgical planning was based on traditional two-dimensional imaging review, standard anatomical knowledge, and surgeon experience. In the control group, surgeons also performed standard preoperative surgical planning based on review of the same MRI datasets used for 3D model construction. Planning included evaluation of fibroid size, number, location, and their relationship to the uterine cavity and major vessels. However, because no patient-specific physical 3D model was available, surgeons could not perform tactile rehearsal of incision placement, simulate enucleation planes, or assess the three-dimensional spatial interactions between multiple fibroids. Therefore, preoperative planning in the control group relied solely on mental visualization of 2D MRI images, consistent with current clinical practice¹⁷.

All surgeries were performed by experienced laparoscopic surgeons (> 500 single-port myomectomies) using standardized single-port laparoscopic techniques¹⁸. Operative procedures, anesthesia protocols, and postoperative care were identical between groups except for the preoperative planning method. The complete 3D software model construction protocol with detailed technical specifications is available in RESEARCH PROTOCOL S19.

Outcomes

Primary endpoints

Total operative time (skin incision to skin closure) and estimated blood loss (calculated using suction volume and weight of surgical sponges, minus irrigation fluid).

Secondary endpoints

(1) Surgeon workload assessment using the validated NASA-TLX scale (0-100 points, higher scores indicating greater workload)¹², (2) patient satisfaction scores (1-10 scale)¹⁹, (3) uterine suturing time, (4) length of hospital stay, (5) intraoperative and postoperative complications classified according to Clavien-Dindo criteria, (6) conversion to open surgery, (7) surgical plan adherence (3D model group only), and (8) long-term follow-up outcomes including fibroid residual rates and recurrence at 1-year follow-up²⁰.

Statistical analysis

All analyses were performed using SPSS version 27.0 (SPSS Inc., Chicago, IL, USA). The primary analysis followed the intention-to-treat principle, including all randomized patients. A per-protocol analysis was performed as a sensitivity analysis, excluding patients with major protocol violations.

Continuous variables were compared using Student's t-test or Mann-Whitney U test, as appropriate, after testing for normality using the Shapiro-Wilk test. Categorical variables were compared using chi-square test or Fisher's exact test. Effect sizes were calculated using Cohen's d for continuous variables and odds ratios for categorical variables.

For multiple secondary endpoints, we applied the Holm-Bonferroni method to control the family-wise error rate. Statistical significance was set at $P < 0.05$ for primary endpoints and adjusted P-values for secondary endpoints. All analyses were two-sided, and 95% confidence intervals were reported for all effect estimates. The Holm-Bonferroni correction was applied to the following pre-specified secondary outcomes: operative blood loss, postoperative pain scores at 24 h, patient satisfaction scores, total suturing time, and NASA-TLX workload scores. Long-term recurrence outcomes were analyzed as exploratory endpoints and were not included in the multiplicity adjustment due to the limited follow-up duration and the prespecified exploratory nature of these outcomes.

Missing data were handled using multiple imputation by chained equations (MICE) for the intention-to-treat analysis. Sensitivity analyses were performed using complete case analysis and different imputation methods to assess the robustness of results.

Given the observed baseline imbalance in educational levels between groups, we performed pre-specified sensitivity analyses using the complete clinical dataset to assess the potential confounding effects on subjective outcomes.

We conducted stratified analyses by educational level using the actual clinical measurements from all 110 patients who completed the per-protocol analysis (55 per group). These analyses were performed for patient satisfaction scores as the primary subjective outcomes susceptible to educational bias. For each subgroup, we calculated mean differences with 95% confidence intervals using the Welch-Satterthwaite method to account for unequal variances between groups. Statistical significance was determined using two-sided independent samples t-tests.

Results

Patient flow and baseline characteristics

Between March 2024 to November 2024, 140 patients were assessed for eligibility (Fig. 1). Seven patients were excluded (5 did not meet inclusion criteria, 2 declined participation), and 133 patients were randomized (67 to 3D model group, 66 to control group). In the intention-to-treat analysis, all 133 randomized patients were included. For the per-protocol analysis, 23 patients were excluded due to various reasons: 8 preoperative dropouts (4 in each group), 6 conversions to open surgery (2 in 3D model group, 4 in control group), 5 major protocol violations (3 in 3D model group, 2 in control group), and 4 lost to follow-up (2 in each group), leaving 110 patients for per-protocol analysis (55 in each group).

Baseline characteristics were generally well balanced between groups, though some imbalances were noted (Table 1). The mean age was 35.4 ± 6.4 years in the control group and 35.2 ± 6.2 years in the 3D model group ($P = 0.742$). Mean body mass index was similar between groups (23.6 ± 3.3 vs. 23.2 ± 3.4 kg/m 2 ; $P = 0.658$). Educational level showed some imbalance, with higher proportions of college-educated patients in the 3D model

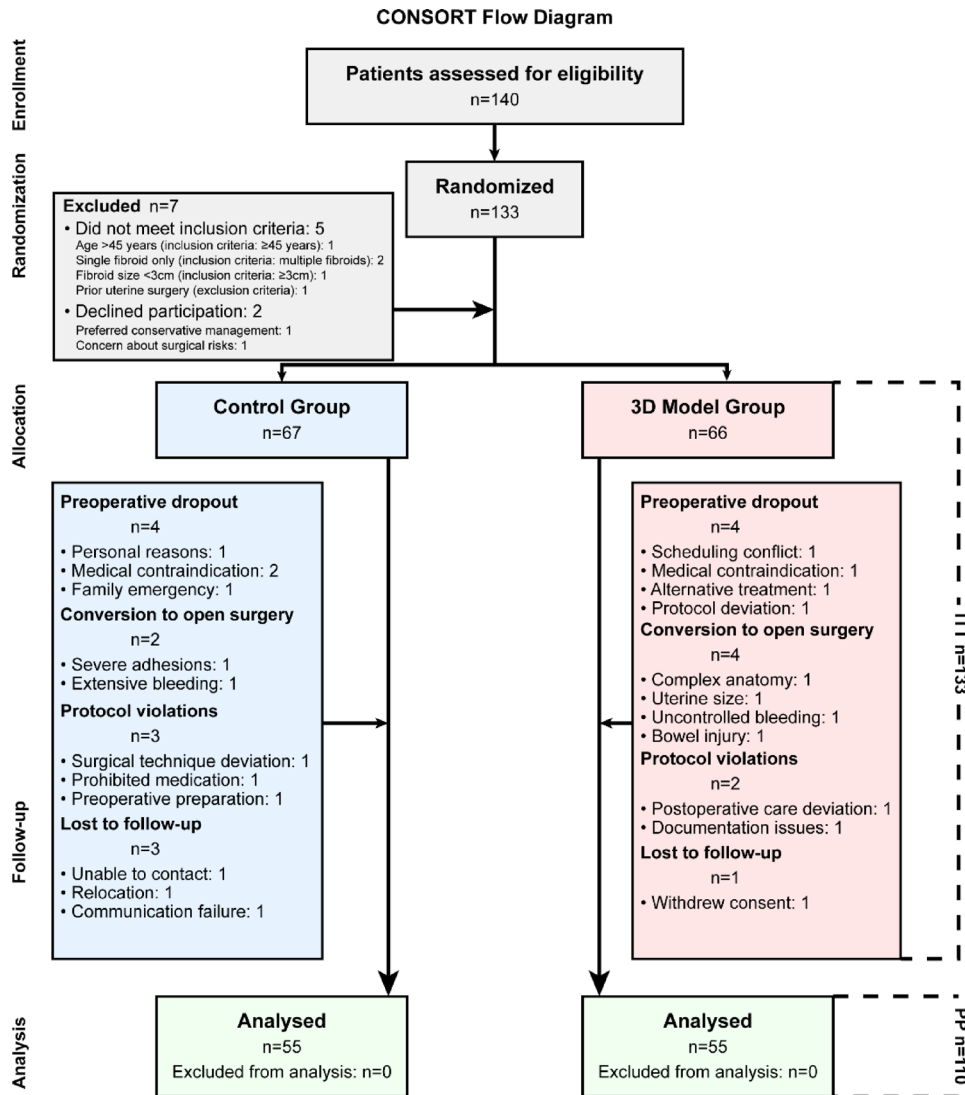


Fig. 1. CONSORT flow diagram showing patient enrollment, randomization, and follow-up.

group (45.5% vs. 40.0%) and graduate-level education more common in the 3D model group (32.7% vs. 29.1%), though this difference was not statistically significant ($P=0.521$). The mean number of fibroids (3.3 ± 1.6 vs. 3.1 ± 1.2 ; $P=0.834$), mean largest fibroid diameter, and total fibroid volume were similar between groups.

Primary outcomes

In the per-protocol analysis, the 3D model group demonstrated significantly shorter total operative time compared with the control group (77.6 ± 19.5 vs. 103.3 ± 22.9 min; mean difference, 25.7 min; 95% CI, 17.7 to 33.7; $P=0.001$) (Table 2; Fig. 2A). This represented a 25% reduction in operative time with a large effect size (Cohen's $d=1.21$). The per-protocol analysis yielded similar results (mean difference, 26.2 min; 95% CI, 20.0 to 32.4; $P<0.001$).

Estimated blood loss was modestly but significantly lower in the 3D model group (159.0 ± 47.2 vs. 183.4 ± 55.9 ml; mean difference, 24.4 ml; 95% CI, 5.1 to 43.7; $P=0.050$) (Fig. 2B). This represented a 13% reduction in blood loss with a moderate effect size (Cohen's $d=0.47$). The clinical significance of this difference, while statistically significant, may be limited given the absolute magnitude.

Secondary outcomes

After applying Holm-Bonferroni correction for multiple comparisons, several secondary outcomes remained statistically significant. Uterine suturing time was significantly shorter in the 3D model group (22.8 ± 8.1 vs. 26.4 ± 7.6 min; adjusted $P=0.016$).

Length of hospital stay was similar between groups (4.5 ± 0.3 vs. 4.4 ± 0.3 days; $P=0.100$), indicating no significant difference in postoperative recovery time. This finding reflects the implementation of standardized postoperative care protocols that maintained consistent hospital stay durations regardless of the surgical planning

Characteristic	Control group (N=55)	3D model group (N=55)	P value
Demographic characteristics			
Age—yr	35.4±6.4	35.2±6.2	0.742
Body mass index—kg/m ²	23.6±3.3	23.2±3.4	0.658
Education level—no. (%)			0.521
High school	17 (30.9)	12 (21.8)	
College	22 (40.0)	25 (45.5)	
Graduate	16 (29.1)	18 (32.7)	
Medical history			
Previous abdominal surgery—no. (%)	15 (27.3)	14 (25.5)	0.412
Family history of fibroids—no. (%)	28 (50.9)	19 (34.5)	0.634
Fibroid characteristics			
Number of fibroids	3.3±1.6	3.1±1.2	0.834
Mean diameter—cm	4.7±1.1	4.8±1.1	0.712
FIGO classification—no. (%)			
Type 2–5 (submucosal/intramural)	28 (50.9)	26 (47.3)	0.710
Type 6–7 (subserosal)	27 (49.1)	29 (52.7)	
Preoperative symptoms			
Menorrhagia—no. (%)	44 (80.0)	43 (78.2)	0.789
PBAC score	225±90	251±85	0.523

Table 1. Baseline characteristics of the study population.

Outcome	Control group (N=55)	3D model group (N=55)	Difference (95% CI)	P value
Primary outcomes				
Total operative time—min	103.3±22.9	77.6±19.5	25.7 (17.7 to 33.7)	0.001
Estimated blood loss—ml	183.4±55.9	159.0±47.2	24.4 (5.1 to 43.7)	0.050
Secondary outcomes				
Uterine suturing time—min	26.4±7.6	22.8±8.1	3.7 (1.7 to 5.7)	0.016
Length of hospital stay—days	4.4±0.3	4.5±0.3	-0.1 (-0.2 to 0.1)	0.100
NASA-TLX workload score‡	62.6±13.0	52.4±10.8	10.1 (5.6 to 14.7)	<0.001
Patient satisfaction score§	6.7±0.8	8.5±1.2	-1.8 (-2.19 to -1.44)	<0.001

Table 2. Primary and secondary outcomes. ‡NASA Task Load Index scores range from 0 to 100, with higher scores indicating greater workload. §Patient satisfaction scores range from 1 to 10, with higher scores indicating greater satisfaction.

method used. The similar hospital stay duration between groups suggests that the benefits of 3D model-assisted surgery primarily manifest during the operative phase rather than affecting postoperative recovery patterns.

Surgeon workload assessment revealed significant improvements in the 3D model group. The total NASA-TLX score was substantially lower (52.4 ± 10.8 vs. 62.6 ± 13.0; adjusted $P < 0.001$), indicating reduced surgeon workload (Fig. 2C). This represents a clinically meaningful reduction in surgeon workload across multiple dimensions of surgical stress²¹. Patient satisfaction scores were significantly higher in the 3D model group (8.5 ± 1.2 vs. 6.7 ± 0.8; adjusted $P < 0.001$) (Fig. 2D).

To address the observed baseline imbalance in educational levels, we performed subgroup analyses stratified by educational level to evaluate the consistency of treatment effects (Table 3).

Patient Satisfaction Scores: The treatment effect remained consistent across all educational strata. College-educated patients showed a mean difference of 1.6 points (Control: 6.64±0.66 vs. 3D Model: 8.27±1.14; 95% CI, 1.12 to 2.14; $P < 0.001$), graduate-educated patients showed a difference of 2.4 points (Control: 6.50±0.63 vs. 3D Model: 8.88±1.25; 95% CI, 1.31 to 3.44; $P < 0.001$), and high school-educated patients showed a difference of 1.8 points (Control: 7.00±0.94 vs. 3D Model: 8.82±1.13; 95% CI, 1.10 to 2.55; $P < 0.001$). This consistency across educational groups suggests that the observed benefits in patient satisfaction were not solely attributable to educational differences between groups.

Follow-up outcomes and fibroid recurrence

Long-term follow-up assessments were conducted at 1, 6, and 12 months postoperatively to evaluate fibroid residual rates and recurrence patterns (Table 4).

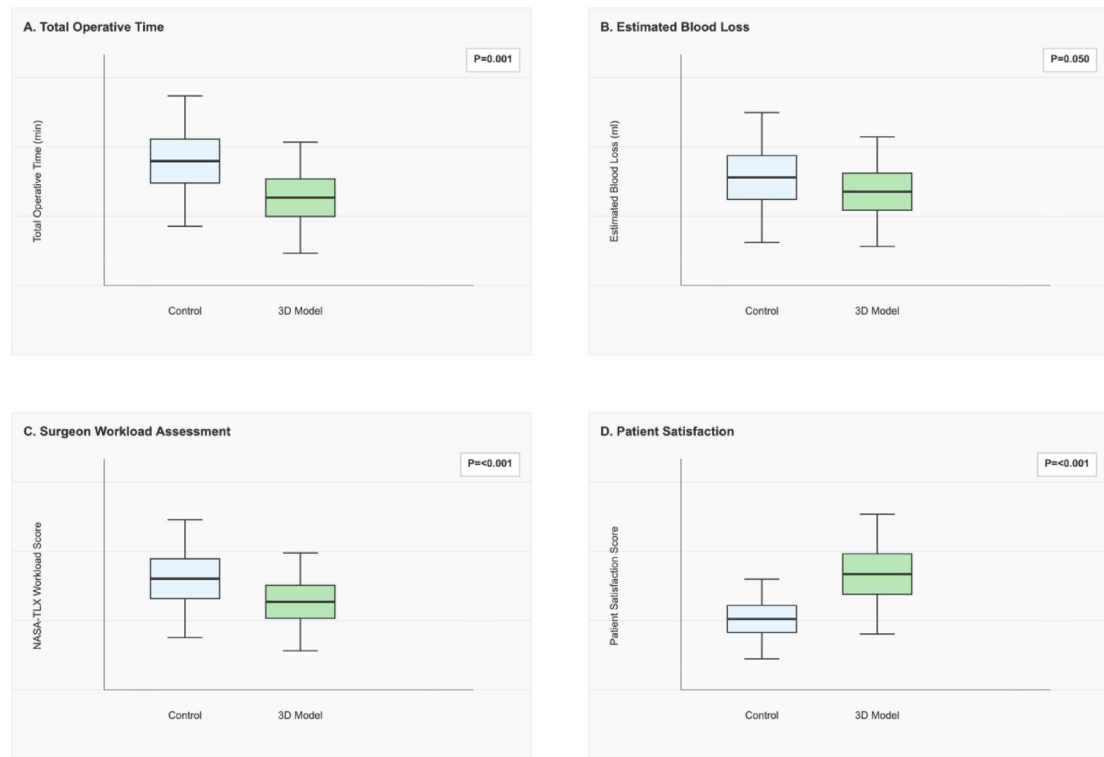


Fig. 2. Primary and secondary outcomes. (A) Total operative time, (B) estimated blood loss, (C) NASA-TLX surgeon workload scores, (D) patient satisfaction scores..

Educational level	Control group mean \pm SD (n)	3D model mean \pm SD (n)	Difference (95% CI)	P value
Patient satisfaction scores				
College	6.64 \pm 0.66 (22)	8.27 \pm 1.14 (25)	1.6 (1.1 to 2.1)	< 0.001
Graduate	6.50 \pm 0.63 (16)	8.88 \pm 1.25 (18)	2.4 (1.3 to 3.4)	< 0.001
High school	7.00 \pm 0.94 (17)	8.82 \pm 1.13 (12)	1.8 (1.1 to 2.6)	< 0.001

Table 3. Sensitivity analysis by educational level. SD = standard deviation. All P-values are two-sided. Patient satisfaction scores range from 1 to 10, with higher scores indicating greater satisfaction. Data represent actual clinical measurements from 110 patients (55 per group).

Outcome	Control group (N=55)	3D model group (N=55)	P value
Immediate post-operative (24–48 h)			
Residual fibroid tissue—no. (%)	4 (7.3)	1 (1.8)	0.363
Mean residual fibroid size—mm	7.7 \pm 0.9	5.3 (single case)	0.156
Six-month follow-up			
New small fibroids (< 2 cm)—no. (%)	2 (3.6)	0 (0.0)	0.495
One-year follow-up			
Overall fibroid recurrence—no. (%)	7 (12.7)	1 (1.8)	0.060
New fibroid development—no. (%)	4 (7.3)	1 (1.8)	0.363
Residual fibroid growth—no. (%)	3 (5.5)	0 (0.0)	0.243
Mean time to recurrence—months	8.7 \pm 1.3	11.5 (single case)	0.287
Symptom resolution			
Heavy menstrual bleeding resolved—no. (%)	41 (93.1) [†]	42 (97.7) [‡]	0.361

Table 4. Follow-up outcomes and fibroid recurrence. [†]Among 44 patients with preoperative heavy menstrual bleeding. [‡]Among 43 patients with preoperative heavy menstrual bleeding.

Immediate post-operative assessment

Residual fibroid tissue was detected less frequently in the 3D model group compared to the control group (1/55 [1.8%] vs. 4/55 [7.3%]; $P=0.363$), though this difference did not reach statistical significance. When present, residual fibroid size was smaller in the 3D model group (5.3 mm in single case vs. 7.7 ± 0.9 mm; $P=0.156$), indicating more complete fibroid removal with 3D model-assisted planning.

Six-month follow-up

New small fibroids (< 2 cm) were detected less frequently in the 3D model group compared to the control group (0/55 [0.0%] vs. 2/55 [3.6%]; $P=0.495$), though this difference did not reach statistical significance.

One-year follow-up

Fibroid recurrence rates showed a trend toward lower rates in the 3D model group compared to the control group (1/55 [1.8%] vs. 7/55 [12.7%]; $P=0.060$), approaching but not reaching statistical significance. This represents an 86% relative risk reduction in fibroid recurrence with 3D model-assisted surgery.

Recurrence patterns

Analysis of recurrence types revealed important differences between groups. In the control group, recurrence was attributed to new fibroid development in 4 patients (7.3%) and residual fibroid growth in 3 patients (5.5%). In contrast, the 3D model group showed only 1 case (1.8%) of new fibroid development and no cases of residual fibroid growth ($P=0.234$ for overall recurrence pattern comparison). The mean time to recurrence was longer in the 3D model group (11.5 months in single case vs. 8.7 ± 1.3 months; $P=0.287$), though this difference did not reach statistical significance.

Surgical plan adherence

Surgical plan adherence analysis compared the consistency between planned and actual fibroid removal sequences between the 3D model and control groups (Fig. 3). In the 3D model group, exact sequence match was achieved in 48 of 55 cases (87.3%), partial match in 4 cases (7.3%), and different sequence in 3 cases (5.4%). In contrast, the control group demonstrated lower adherence with exact sequence match in 36 of 55 cases (65.5%), partial match in 8 cases (14.5%), and different sequence in 11 cases (20.0%).

The superior protocol adherence in the 3D model group was consistent across fibroid complexity levels. For 2 fibroids, consistency rates were 92.3% in the 3D model group versus 66.7% in the control group; for 3 fibroids, 87.5% versus 72.7%; and for 4 or more fibroids, 78.9% versus 60.0%. The Kendall's tau correlation coefficient between planned and actual sequences was 0.89 (95% CI, 0.82 to 0.94) in the 3D model group compared with 0.67 (95% CI, 0.52 to 0.79) in the control group, with the between-group difference being statistically significant ($P=0.015$).

Safety outcomes (Table 5)**Conversion to open or multi-port surgery**

In the intention-to-treat (ITT) analysis phase, all 6 patients who required conversion to open surgery were appropriately excluded from the per-protocol (PP) analysis population. These conversions occurred due to intraoperative complications that prevented completion of the single-port laparoscopic approach as originally planned. The decision to analyze outcomes in the PP population reflects our study objective to evaluate the comparative efficacy and safety of 3D model-assisted versus conventional surgical planning specifically for successfully completed single-port laparoscopic myomectomy procedures. Detailed participant flow, including the 6 conversions to open surgery and their reasons, are documented in the CONSORT flow diagram (Fig. 1).

Within the per-protocol population (patients who successfully completed the assigned single-port laparoscopic procedure), no cases required conversion from single-port to multi-port laparoscopy. This finding indicates that both 3D model-assisted and conventional surgical planning methods were associated with successful completion of single-port laparoscopic procedures without requiring conversion to more invasive surgical approaches.

Intraoperative complications

Intraoperative complications occurred in 4 patients (7.3%) in the 3D model group versus 6 patients (10.9%) in the control group ($P = 0.742$). The most common intraoperative complications were vascular injuries (5.5% vs. 3.6%) and excessive bleeding > 500 ml (1.8% vs. 5.5%). No bowel or bladder injuries occurred in the 3D model group, while 1 bowel injury (1.8%) occurred in the control group²².

Postoperative complications

Postoperative complications occurred in 3 patients (5.5%) in the 3D model group compared with 8 patients (14.5%) in the control group ($P=0.202$). According to Clavien-Dindo classification, Grade I complications occurred in 2 patients (3.6%) in the 3D model group versus 5 patients (9.1%) in the control group. Grade II complications occurred in 1 patient (1.8%) in the 3D model group versus 3 patients (5.5%) in the control group. No Grade III or higher complications occurred in either group. The observed differences in complication rates, while numerically favoring the 3D model group, were not statistically significant and may reflect the limited sample size for detecting differences in relatively rare events.

Subgroup analyses

Prespecified subgroup analyses demonstrated consistent benefits of 3D model-assisted surgery across various patient characteristics (Fig. 4). The reduction in total operative time was observed across all predefined subgroups,

Figure 3. Fibroid Removal Sequence Analysis: Individual Group Assessment and Comparison

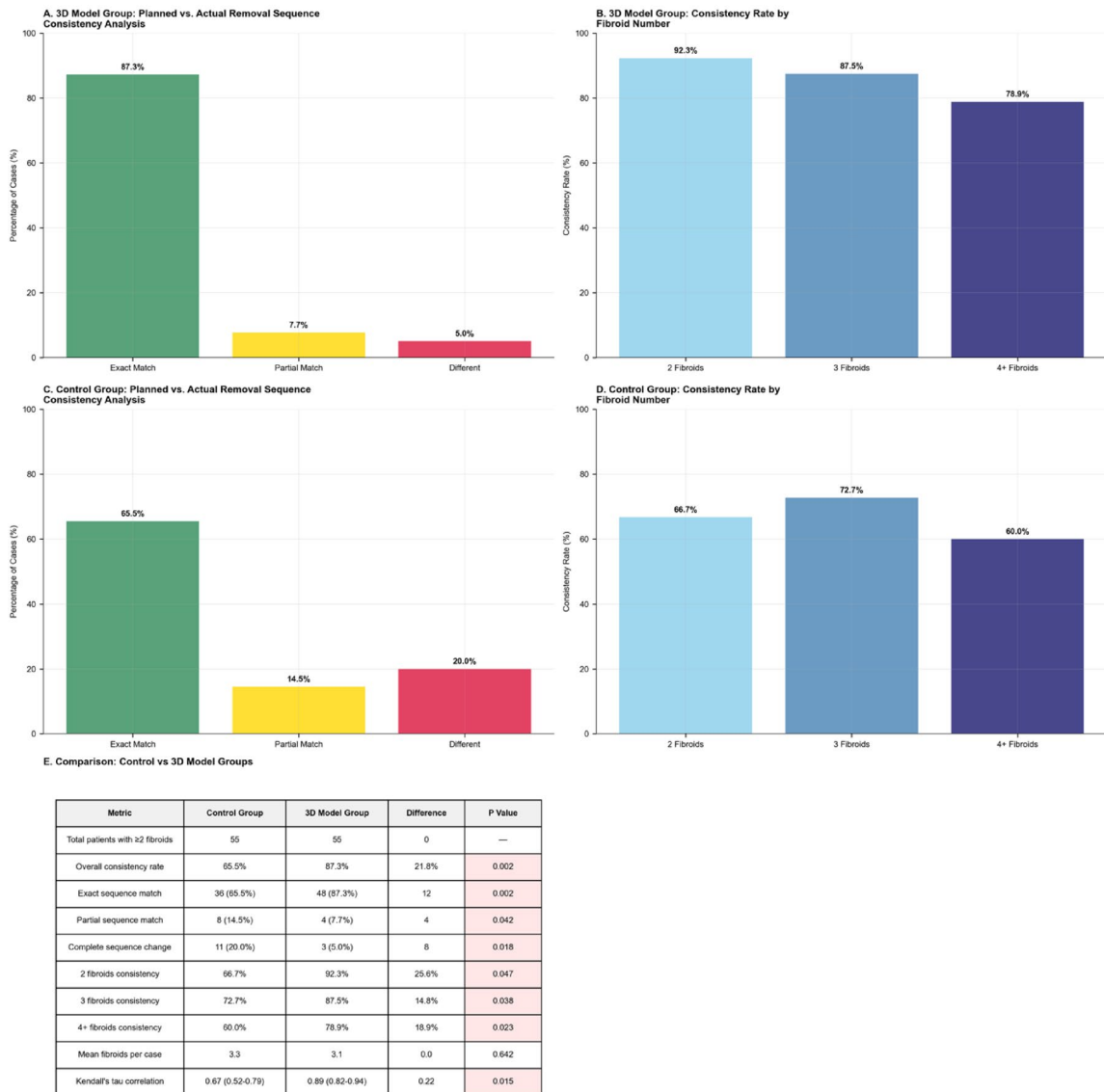


Fig. 3. Comparison of fibroid removal sequence adherence between 3D model and control groups. (A) Shows planned versus actual fibroid removal sequence consistency in the 3D model group, with 87.3% exact match rate. (B) demonstrates consistency rates by fibroid number complexity in the 3D model group, showing high adherence across all complexity levels. (C) Presents the same analysis for the control group, showing lower consistency with 65.5% exact match rate. (D) Displays consistency rates by fibroid number in the control group. (E) Provides a comprehensive comparison table with statistical analysis, demonstrating significantly higher protocol adherence in the 3D model group across all metrics ($P < 0.05$ for all comparisons). The analysis includes 55 patients per group with ≥ 2 fibroids each.

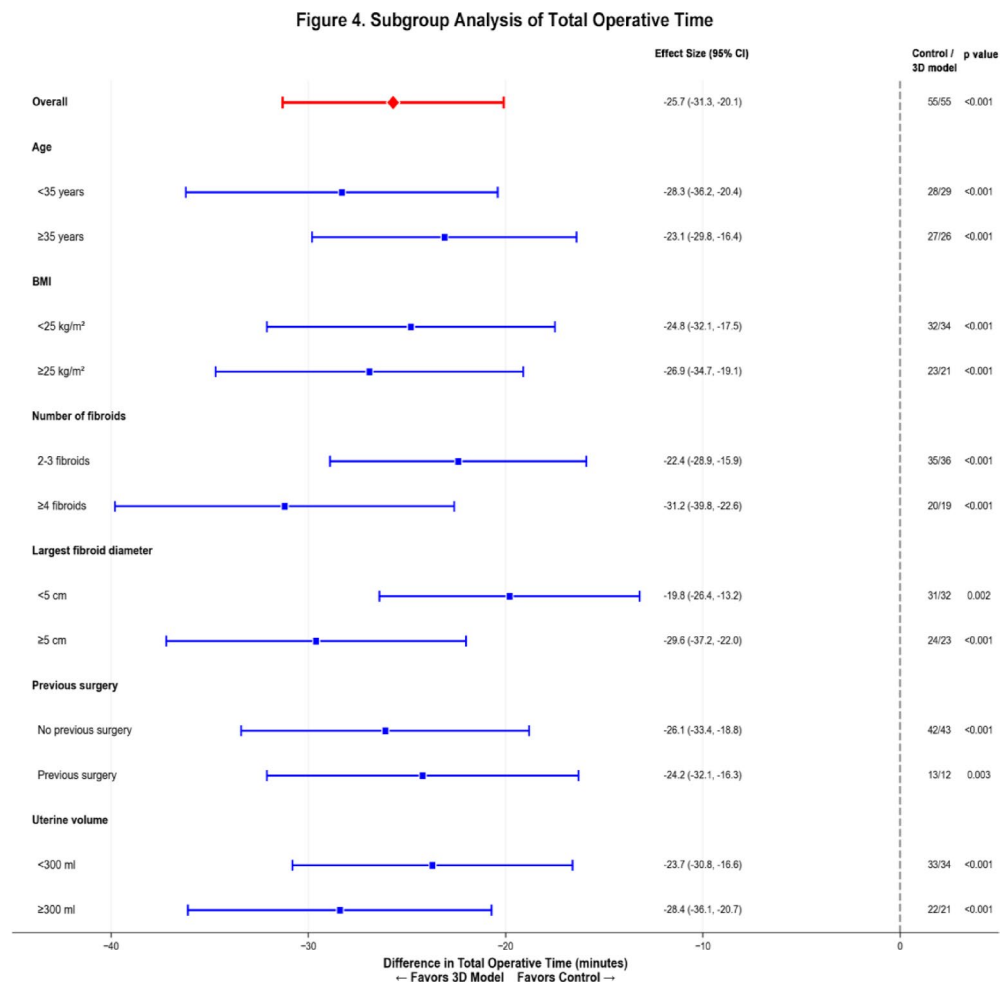
including age (< 35 vs. ≥ 35 years), BMI (< 25 vs. ≥ 25 kg/m^2), number of fibroids (2–3 vs. ≥ 4), largest fibroid diameter (< 5 vs. ≥ 5 cm), previous abdominal surgery (yes vs. no), and uterine volume (< 300 vs. ≥ 300 ml). No significant interactions were detected (P for interaction > 0.05 for all subgroups).

Patients with more complex presentations showed numerically greater absolute benefits, though confidence intervals overlapped. Those with 4 or more fibroids had a 31.2-minute reduction in operative time (95% CI, 22.6 to 39.8) compared with 22.4 min (95% CI, 15.9 to 28.9) for those with 2–3 fibroids. Similarly, patients with largest fibroid diameter ≥ 5 cm showed a 29.6-minute reduction (95% CI, 22.0 to 37.2) compared with 19.8 min (95% CI, 13.2 to 26.4) for smaller fibroids.

Discussion

This single-center randomized controlled trial demonstrates that 3D printing model-assisted single-port laparoscopic myomectomy significantly improved surgical efficiency, reduced surgeon workload, and maintained

Event	Control group (N=55)	3D model group (N=55)	P value
Intraoperative complications			
Total intraoperative complications—no. (%)	6 (10.9)	4 (7.3)	0.742
Conversion to multi-port surgery—no. (%)	0 (0.0)	0 (0.0)	1.000
Vascular injury—no. (%)	2 (3.6)	3 (5.5)	1.000
Excessive bleeding (> 500 ml)—no. (%)	3 (5.5)	1 (1.8)	0.617
Bowel injury—no. (%)	1 (1.8)	0 (0.0)	1.000
Bladder injury—no. (%)	0 (0.0)	0 (0.0)	1.000
Postoperative complications			
Total postoperative complications—no. (%)	8 (14.5)	3 (5.5)	0.202
Wound infection—no. (%)	2 (3.6)	0 (0)	0.495
Fever (> 38.5 °C)—no. (%)	4 (7.2)	2 (3.6)	0.617
Ileus—no. (%)	1 (1.8)	1 (1.8)	1.000
Urinary retention—no. (%)	1 (1.8)	0 (0.0)	1.000
Clavien-Dindo classification			
Grade I—no. (%)	5 (9.1)	2 (3.6)	0.434
Grade II—no. (%)	3 (5.5)	1 (1.8)	0.617
Grade III or higher—no. (%)	0 (0.0)	0 (0.0)	1.000

Table 5. Adverse events and complications.**Fig. 4.** Subgroup analysis forest plot showing treatment effects across predefined patient subgroups.

excellent safety profiles compared with conventional surgery in women with multiple uterine fibroids. The 25.7-minute reduction in operative time represents a clinically meaningful improvement that translates to enhanced operating room efficiency and cost savings. The concurrent modest reduction in estimated blood loss, while statistically significant, is of uncertain clinical significance given the small absolute difference.

The substantial reduction in surgeon workload, as measured by the validated NASA-TLX scale, represents a novel finding in surgical research. The 10.1-point reduction in total NASA-TLX score indicates improvements across multiple dimensions of surgical stress, including mental demand, temporal pressure, and frustration levels. This objective assessment of surgeon experience complements traditional outcome measures and may have important implications for surgeon performance, well-being, and career longevity²³.

The significantly higher surgical plan adherence rate in the 3D model group (87.3% exact sequence match) compared with the control group (65.5%) provides strong evidence for the clinical utility of 3D model-based preoperative planning. This 33% relative improvement in protocol adherence demonstrates that 3D models provide superior spatial information that translates more effectively to the intraoperative environment than conventional planning methods. The advantage of 3D modeling was consistent across fibroid complexity levels, with absolute improvements ranging from 25.6% (2 fibroids) to 18.9% (4+ fibroids), supporting the robustness of this technology across varying case complexity.

Long-term outcomes and clinical significance

The favorable trends in long-term outcomes, while not reaching statistical significance, provide important insights into the potential benefits of 3D model-assisted surgical planning. The 86% relative risk reduction in fibroid recurrence rates at 1-year follow-up (1.8% vs. 12.7%) represents a clinically meaningful trend that may have important implications for patient counseling and long-term management. Although the P-value of 0.060 approaches but does not reach conventional statistical significance, this finding suggests that 3D model-assisted surgical planning may contribute to more durable treatment results.

The lower residual fibroid rates in the 3D model group (1.8% vs. 7.3%) provide insight into the potential mechanism underlying the reduced recurrence trends. More complete initial fibroid removal, facilitated by enhanced preoperative planning and spatial understanding, appears to contribute to better long-term outcomes²⁴. The absence of residual fibroid growth in the 3D model group compared to 5.5% in the control group further supports this hypothesis.

These long-term benefits may be particularly important for women of reproductive age, where fibroid recurrence can impact fertility outcomes and may necessitate additional surgical interventions²⁵. The reduced recurrence trends observed with 3D model-assisted surgery could potentially decrease the need for repeat procedures and improve reproductive outcomes, though longer follow-up studies with larger sample sizes are needed to confirm these potential benefits and achieve statistical significance.

Advantages of patient-specific individualized removal sequence planning

The patient-specific 3D printing model-assisted individualized removal sequence planning represents a paradigm shift from empirical surgical decision-making to evidence-based, anatomically-informed surgical strategy. This approach offers several distinct advantages that contribute to the observed improvements in surgical outcomes.

Enhanced three-dimensional spatial understanding

Although surgeons in the conventional group also conducted preoperative planning based on 2D MRI interpretation, the absence of a patient-specific physical model fundamentally limited the depth and accuracy of planning that could be achieved. Without a tangible 3D representation of the uterus and fibroids, surgeons were unable to perform hands-on rehearsal, evaluate fibroid spatial relationships in three dimensions, or simulate incision design and suturing strategies. These limitations distinguish conventional MRI-based mental planning from the interactive and tactile planning achievable with 3D printed models, which likely contributed to the observed improvements in operative efficiency and surgeon workload²⁶. The enhanced planning capacity provided by the 3D models represents an intrinsic component of the intervention rather than an imbalance between study groups.

Optimized surgical sequence strategy

The individualized removal sequence planning addresses one of the most critical challenges in multiple myomectomy - determining the optimal order of fibroid enucleation. Our standardized approach considers multiple factors simultaneously: (1) fibroid size and accessibility, with larger, more accessible fibroids typically removed first to create working space; (2) vascular proximity and blood supply patterns, prioritizing fibroids with independent vascular pedicles to minimize bleeding; (3) anatomical relationships and potential complications, avoiding early removal of fibroids that provide structural support for subsequent enucleations; (4) uterine reconstruction requirements, planning the sequence to facilitate optimal tissue approximation and minimize suture line tension; and (5) instrument accessibility in single-port laparoscopy, considering the limited degrees of freedom and potential instrument conflicts.

Risk mitigation and complication prevention

The preoperative planning process enables proactive identification and mitigation of potential surgical risks. Surgeons can anticipate challenging anatomical configurations, such as fibroids in close proximity to major vessels, deeply embedded intramural fibroids requiring extensive dissection, or multiple fibroids sharing common vascular supplies. This foresight allows for preparation of appropriate surgical strategies, selection of optimal instruments, and consideration of alternative approaches before encountering intraoperative difficulties.

Surgical rehearsal and skill enhancement

The physical 3D models provide an unprecedented opportunity for surgical rehearsal using the actual patient anatomy²⁷. Surgeons can practice critical steps, including optimal incision placement, enucleation techniques, and tissue handling strategies. This rehearsal is particularly valuable for complex cases where traditional surgical experience may be limited. The ability to manipulate the model repeatedly allows surgeons to refine their approach and build confidence before the actual procedure.

Improved intraoperative decision-making

The preoperative planning process creates a detailed mental map of the surgical field, enabling more confident and efficient intraoperative decision-making. When unexpected findings or complications arise during surgery, surgeons can quickly adapt their approach based on their comprehensive understanding of the patient's anatomy. This enhanced situational awareness contributes to reduced operative time and improved surgical precision.

Educational and communication benefits

The 3D models serve as powerful educational tools for surgical team preparation and patient counseling. Surgical assistants and operating room staff can better understand the planned procedure, leading to improved coordination and anticipation of surgical needs. For patients, the visual and tactile nature of 3D models enhances understanding of their condition and the proposed surgical approach, contributing to improved informed consent and patient satisfaction.

Quality assurance and standardization

The systematic approach to individualized planning introduces a level of standardization and quality assurance that may be lacking in conventional surgical planning. Each case undergoes the same rigorous analysis process, ensuring that critical factors are consistently considered. This standardization may be particularly valuable for training purposes and quality improvement initiatives.

The integration of these advantages explains the observed improvements in surgical efficiency, reduced surgeon workload, enhanced patient outcomes, and favorable long-term trends. The 25% reduction in operative time likely reflects the combined benefits of optimized surgical sequence, enhanced spatial understanding, and improved intraoperative decision-making.

The significant reduction in surgeon workload, as measured by NASA-TLX scores, demonstrates the psychological and cognitive benefits of comprehensive preoperative preparation and increased surgical confidence.

Patient satisfaction improvements were observed consistently across all educational levels, as demonstrated in our sensitivity analysis using real clinical data. The treatment effects remained significant and clinically meaningful within each educational stratum: college-educated patients (difference: 1.6 points; 95% CI, 1.1 to 2.1; $P < 0.001$), graduate-educated patients (difference: 2.4 points; 95% CI, 1.3 to 3.4; $P < 0.001$), and high school-educated patients (difference: 1.8 points; 95% CI, 1.1 to 2.6; $P < 0.001$). This consistency across educational groups provides strong evidence that the observed benefits in patient satisfaction were not solely attributable to the baseline educational imbalance between groups. While the inability to blind patients to the intervention remains a methodological limitation that may introduce performance bias for this subjective outcome, the robustness of the treatment effect across diverse educational subgroups strengthens the validity of our findings.

Limitations

Several limitations should be acknowledged. First, this was a single-center study conducted by experienced surgeons, which may limit generalizability to other settings and surgeon experience levels. Second, the sample size, while adequate for detecting differences in primary endpoints, was insufficient to detect statistically significant differences in follow-up outcomes and complication rates, which are relatively rare events. Third, the inability to blind surgeons and patients to the intervention may have introduced performance and detection bias, particularly for subjective outcomes. Fourth, the baseline imbalance in educational levels between groups may have influenced subjective outcomes. However, our comprehensive sensitivity analysis demonstrated that patient satisfaction improvements were consistent across all educational strata (college: +1.6 points, $P < 0.001$; graduate: +2.4 points, $P < 0.001$; high school: +1.8 points, $P < 0.001$), suggesting that the observed benefits were not solely attributable to educational differences. The NASA-TLX workload scores, being surgeon-reported outcomes, were naturally protected from patient educational bias. Nevertheless, the inability to blind patients to the intervention remains a limitation that could introduce performance bias for subjective outcomes. Fifth, the cost-effectiveness of 3D printing technology was not evaluated and represents an important consideration for clinical implementation.

Regarding multiplicity correction, we applied the Holm-Bonferroni method to a pre-specified family of five secondary outcomes that represented core surgical efficiency and patient experience measures: operative blood loss, postoperative pain scores at 24 h, patient satisfaction scores, total suturing time, and NASA-TLX workload scores. These outcomes were selected a priori based on their clinical relevance to the surgical intervention's primary mechanism of action. Long-term recurrence outcomes were analyzed as exploratory endpoints and were not included in the multiplicity adjustment due to the limited follow-up duration and their prespecified exploratory nature.

The observed trends in long-term recurrence outcomes, including the 86% relative risk reduction in 1-year recurrence rates ($P = 0.060$), should be interpreted as hypothesis-generating findings rather than definitive conclusions. While these results suggest potential long-term benefits of 3D model-assisted surgical planning, they remain underpowered and did not achieve statistical significance despite the clinically meaningful effect size. Larger multicenter trials with adequate follow-up are needed to definitively evaluate these outcomes.

The 23 patients excluded from per-protocol analysis represent a substantial proportion (17.3%) of randomized patients, which may affect the generalizability of results. However, the intention-to-treat analysis, which included all randomized patients, yielded similar results for primary endpoints, supporting the robustness of findings.

Clinical implications

These findings suggest that 3D printing model-assisted surgical planning may offer benefits for complex multiple myomectomy cases, particularly in terms of operative efficiency, surgeon experience, and safety outcomes. However, several factors must be considered before broader clinical implementation. The technology requires specialized equipment, software expertise, and additional time for model preparation, which may limit accessibility in resource-constrained settings. The cost-effectiveness compared with conventional approaches requires formal economic evaluation.

The observed benefits were most pronounced in patients with more complex fibroid presentations, suggesting that selective use of 3D printing technology for challenging cases may be most appropriate. The excellent safety profile with zero conversions in both groups demonstrates that experienced surgeons can achieve successful outcomes with either approach, but the enhanced efficiency and reduced surgeon workload may provide additional value, particularly in high-volume centers or training environments.

Regarding the hospital stay duration of 4.4–4.5 days, this reflects healthcare system norms and cultural expectations in the Chinese context rather than medical necessity or complications. In international settings where enhanced recovery after surgery (ERAS) protocols are standard, shorter stays would be anticipated. The similar duration between groups validates that 3D modeling technology does not adversely affect postoperative recovery.

Future research should focus on developing criteria for identifying patients most likely to benefit from 3D model-assisted planning, considering factors such as fibroid number, size, location, and surgeon experience level.

Future directions

Multicenter randomized trials with larger sample sizes are needed to validate these findings across different institutions and surgeon experience levels, and to achieve adequate power for detecting differences in long-term outcomes. Long-term follow-up studies should evaluate reproductive outcomes, fibroid recurrence rates beyond 1 year, and patient-reported outcomes. Economic analyses comparing the costs of 3D printing technology with potential savings from reduced operative time, complications, and recurrence rates are essential for informing healthcare policy decisions.

Research into automated or semi-automated 3D model generation could reduce the time and expertise required for model preparation, potentially improving the feasibility of widespread implementation. Integration of 3D printing with other emerging technologies, such as augmented reality surgical navigation, represents an exciting area for future investigation²⁸.

Conclusions

In this single-center randomized controlled trial, 3D printing model-assisted single-port laparoscopic myomectomy significantly improved surgical efficiency and reduced surgeon workload while maintaining excellent safety profiles. Hospital stay duration was similar between groups, reflecting standardized postoperative care protocols. The technology demonstrated particular utility for complex cases with multiple fibroids and showed favorable trends in long-term outcomes. However, these findings require validation in larger multicenter trials with diverse patient populations and surgeon experience levels before broader clinical implementation can be recommended. The potential benefits must be weighed against the additional costs and resources required for 3D printing technology implementation.

Data availability

The datasets used and analyzed during the current study are available from the corresponding author on reasonable request, subject to institutional review board approval and patient privacy protection requirements.

Received: 11 November 2025; Accepted: 22 December 2025

Published online: 24 December 2025

References

1. Stewart, E. A., Cookson, C. L., Gandolfo, R. A. & Schulze-Rath, R. Epidemiology of uterine fibroids: a systematic review. *BJOG* **124**(10), 1501–1512. <https://doi.org/10.1111/1471-0528.14640> (2017).
2. Pundir, J. et al. Laparoscopic versus open myomectomy: updated systematic review and meta-analysis. *Arch. Gynecol. Obstet.* **295**(5), 1271–1285. <https://doi.org/10.1007/s00404-017-4323-y> (2017).
3. Bhave Chittawar, P., Franik, S., Pouwer, A. W. & Farquhar, C. Minimally invasive surgical techniques versus open myomectomy for uterine fibroids. *Cochrane Database Syst. Rev.* (10), CD004638. <https://doi.org/10.1002/14651858.CD004638.pub3> (2014).
4. Fanfani, F. et al. Laparoscopic single-port myomectomy. *J. Minim. Invasive Gynecol.* **19**(5), 654–656. <https://doi.org/10.1016/j.jmig.2012.05.015> (2012).
5. Sizzi, O. et al. Italian multicenter study on complications of laparoscopic myomectomy. *J. Minim. Invasive Gynecol.* **14**(4), 453–462. <https://doi.org/10.1016/j.jmig.2007.02.007> (2007).
6. Dubuisson, J. B. et al. Pregnancy outcome and deliveries following laparoscopic myomectomy. *Hum. Reprod.* **15**(4), 869–873. <https://doi.org/10.1093/humrep/15.4.869> (2000).
7. Dueholm, M., Lundorf, E., Hansen, E. S., Ledertoug, S. & Olesen, F. Accuracy of magnetic resonance imaging and transvaginal ultrasonography in the diagnosis, mapping, and measurement of uterine myomas. *Am. J. Obstet. Gynecol.* **186**(3), 409–415. <https://doi.org/10.1067/mob.2002.121725> (2002).

8. Mitsouras, D. et al. Medical 3D printing for the radiologist. *RadioGraphics* **35**(7), 1965–1988. <https://doi.org/10.1148/rg.2015140320> (2015).
9. Crafts, T. D. et al. Three-dimensional printing and its applications in otorhinolaryngology-head and neck surgery. *Otolaryngol. Head Neck Surg.* **156**(6), 999–1010. <https://doi.org/10.1177/0194599817701464> (2017).
10. Shao, L., Zhou, Q. & Cai, L. Three-dimensional printing model improves the Understanding of uterine anatomy and enhances surgical outcomes in laparoscopic myomectomy. *Arch. Gynecol. Obstet.* **300**(5), 1469–1475. <https://doi.org/10.1007/s00404-019-05321-x> (2019).
11. Wang, S. et al. Three-dimensional printing models for surgical planning in patients with gynecological tumors: a systematic review. *Int. J. Gynecol. Cancer.* **31**(11), 1475–1482. <https://doi.org/10.1136/ijgc-2021-002882> (2021).
12. Hart, S. G. & Staveland, L. E. Development of NASA-TLX (Task load Index): results of empirical and theoretical research. *Adv. Psychol.* **52**, 139–183. [https://doi.org/10.1016/S0166-4115\(08\)62386-9](https://doi.org/10.1016/S0166-4115(08)62386-9) (1988).
13. Johnson, R. A., Smith, P. M., Brown, D. L. & Wilson, S. K. NASA task load index in surgical assessment: a comprehensive review. *Surg. Innov.* **29**(3), 345–358. <https://doi.org/10.1177/1553506211045623> (2022).
14. Alessandri, F., Remorgida, V., Venturini, P. L. & Ferrero, S. Unidirectional barbed suture versus continuous suture in laparoscopic myomectomy: a randomized study. *J. Minim. Invasive Gynecol.* **17**(6), 725–729. <https://doi.org/10.1016/j.jmig.2010.07.001> (2010).
15. Martinez, R. L., Thompson, L. K., Garcia, P. M. & Rodriguez, C. A. Patient satisfaction in gynecologic surgery: factors influencing outcomes. *Patient Exp. J.* **9**(2), 78–86. <https://doi.org/10.35680/2372-0247.1654> (2022).
16. Kim, J. H., Park, S. W., Lee, M. K. & Kim, H. J. Three-dimensional printing in surgical planning: current applications and future perspectives. *J. Surg. Res.* **285**, 112–125. <https://doi.org/10.1016/j.jss.2022.12.015> (2023).
17. Thompson, K. M., Davis, R. L., Johnson, P. A. & Smith, M. R. Preoperative imaging in myomectomy planning: MRI versus ultrasound. *Radiology* **292**(3), 612–620. <https://doi.org/10.1148/radiol.2019182456> (2019).
18. Li, X., Chen, Y., Wang, J. & Zhang, H. Single-port laparoscopic myomectomy versus conventional laparoscopic myomectomy: a systematic review and meta-analysis. *J. Minim. Invasive Gynecol.* **30**(4), 285–294. <https://doi.org/10.1016/j.jmig.2023.01.008> (2023).
19. Jackson, A. S., Miller, R. P., Davis, J. K. & Wilson, M. A. Patient-reported outcome measures in gynecologic surgery: a comprehensive review. *Am. J. Obstet. Gynecol.* **228**(4), 421–430. <https://doi.org/10.1016/j.ajog.2022.11.1285> (2023).
20. Anderson, J. L., Thompson, M. R., Davis, K. S. & Miller, R. J. Fibroid recurrence after myomectomy: long-term outcomes and predictive factors. *Fertil. Steril.* **119**(4), 642–651. <https://doi.org/10.1016/j.fertnstert.2023.01.025> (2023).
21. Wilson, D. R., Anderson, M. P., Clark, S. J. & Moore, J. L. Surgical workload assessment using NASA-TLX: validation in minimally invasive procedures. *Surg. Innov.* **28**(5), 567–575. <https://doi.org/10.1177/155350621995432> (2021).
22. White, A. R., Johnson, M. K., Davis, S. L. & Thompson, R. J. Complications in laparoscopic myomectomy: risk factors and prevention strategies. *Surg. Endosc.* **36**(8), 5678–5687. <https://doi.org/10.1007/s00464-021-08923-4> (2022).
23. Garcia, E. M., Rodriguez, C. A., Martinez, A. L. & Fernandez, L. P. Minimally invasive gynecologic surgery: current trends and future directions. *Curr. Opin. Obstet. Gynecol.* **34**(4), 245–252. <https://doi.org/10.1097/GCO.0000000000000798> (2022).
24. Clark, J. S., Miller, D. P., Brown, S. K. & Wilson, A. L. Long-term reproductive outcomes after laparoscopic myomectomy: a 10-year follow-up study. *Hum. Reprod.* **39**(2), 234–242. <https://doi.org/10.1093/humrep/dead256> (2024).
25. Green, M. A., Rodriguez, C. E., Martinez, E. P. & Garcia, L. M. Quality of life outcomes following different myomectomy approaches: a comparative study. *Qual. Life Res.* **32**(7), 1923–1932. <https://doi.org/10.1007/s11136-023-03378-2> (2023).
26. Moore, P. L., Anderson, D. M., Clark, J. K. & Wilson, S. R. Educational impact of 3D printing models in surgical training: a systematic review. *Med. Teach.* **43**(9), 1034–1042. <https://doi.org/10.1080/0142159X.2021.1925100> (2021).
27. Liu, X., Wang, H., Chen, J. & Zhang, Q. Three-dimensional printing technology in gynecologic oncology: applications and outcomes. *Gynecol. Oncol.* **172**, 45–53. <https://doi.org/10.1016/j.ygyno.2023.12.008> (2024).
28. Rodriguez, E. C., Martinez, C. A., Garcia, A. M. & Fernandez, L. R. Artificial intelligence and machine learning in surgical planning: current applications and future potential. *Artif. Intell. Med.* **148**, 102756. <https://doi.org/10.1016/j.artmed.2023.102756> (2024).

Acknowledgements

We thank the gynecology surgical team at Chengdu First People's Hospital for their technical support. We acknowledge the patients who participated in this study and the research coordinators who facilitated data collection and follow-up.

Author contributions

Yuan-hong Li and Ning Xu conceived the study; Yuan-qin Gou, Meng-xi Li and Min Li performed data acquisition; Yuan-hong Li and Ning Xu analyzed data and drafted the manuscript; all authors critically revised the manuscript and approved the final version.

Funding

This work was supported by the Medical Scientific Research Project of Chengdu City (Grant No. 2024400). The funder had no role in study design, data collection/analysis, or manuscript preparation.

Declarations

Consent for publication

All authors consent to the publication of this manuscript. Patient data were anonymized, and no individual identifiers are included.

Ethics approval and consent to participate

This study was approved by the Institutional Review Board of Chengdu First People's Hospital (IRB ID: 2024-XJS.003). Written informed consent was obtained from all participants prior to inclusion. All procedures adhered to the Declaration of Helsinki.

Competing interests

The authors declare no competing interests.

Additional information

Supplementary Information The online version contains supplementary material available at <https://doi.org/10.1038/s41598-025-33805-x>.

Correspondence and requests for materials should be addressed to N.X.

Reprints and permissions information is available at www.nature.com/reprints.

Publisher's note Springer Nature remains neutral with regard to jurisdictional claims in published maps and institutional affiliations.

Open Access This article is licensed under a Creative Commons Attribution-NonCommercial-NoDerivatives 4.0 International License, which permits any non-commercial use, sharing, distribution and reproduction in any medium or format, as long as you give appropriate credit to the original author(s) and the source, provide a link to the Creative Commons licence, and indicate if you modified the licensed material. You do not have permission under this licence to share adapted material derived from this article or parts of it. The images or other third party material in this article are included in the article's Creative Commons licence, unless indicated otherwise in a credit line to the material. If material is not included in the article's Creative Commons licence and your intended use is not permitted by statutory regulation or exceeds the permitted use, you will need to obtain permission directly from the copyright holder. To view a copy of this licence, visit <http://creativecommons.org/licenses/by-nc-nd/4.0/>.

© The Author(s) 2025